Impact of Negative Camber for Performance of Vertical Axis Wind Turbine

Abotaleb, Basem
Aerospace Engineering, Cairo University

Mohamed. M. Takeyeldein
Faculty of Engineering, King Salman International University

Huzayyin, Omar
Mechanical Engineering, Cairo University

Elhadidi, Basman
Mechanical and Aerospace Engineering, Nazarbayev University

https://doi.org/10.5109/7172281

出版情報：Evergreen. 11 (1), pp.286-294, 2024-03. 九州大学グリーンテクノロジー研究教育センター
バージョン：

Impact of Negative Camber for Performance of Vertical Axis Wind Turbine

Basem Abotaleb[1], Mohamed. M. Takeyeldein[2,*], Omar Huzayyin[3], Basman Elhadidi[4]

[1] Aerospace Engineering, Cairo University, Egypt

[2]Faculty of Engineering, King Salman International University, Egypt

[3]Mechanical Engineering, Cairo University, Egypt

[4]Mechanical and Aerospace Engineering, Nazarbayev University, Kazakhstan

*Author to whom correspondence should be addressed:
E-mail: mohamed.takey@ksiu.edu.eg

(Received August 01, 2023: Revised January 12, 2024: Accepted January 22, 2024).

Abstract: Vertical axis wind turbines are often best suited for urban areas with limited space and turbulent wind flows. This study examined the impact of airfoil shape on the performance of an H-Darrieus wind turbine using Computational Fluid Dynamics (CFD) modeling. As wake and blade interactions are significant for VAWTs, an unsteady simulation with a sliding mesh was used for all simulations. The models show that achieving a quasi-steady state solution for the VAWT requires at least 50 revolutions to fully account for the unsteady wake interactions with the blades. The CFD results confirmed that a negatively cambered airfoil does not improve the overall efficiency or power coefficient of a VAWT compared to a symmetric or positively cambered airfoil section. The analysis shows that in the first half of the VAWT cycle, the turbine with a negatively cambered airfoil produces an average torque that is 8.8% higher. However, in the second half of the cycle, the turbine with a positively cambered airfoil generates an average negative torque that is 118% lower. As a result, it is recommended to use an adaptive cambered airfoil profile that can optimize performance over the entire cycle.

Keywords: Wind turbine aerodynamics; Vertical Axis wind turbines; negative camber airfoils; H-Darrius turbines.

1. Introduction

Wind turbine use is the fastest-growing renewable energy resource as it converts wind energy to electric energy without emitting pollutants [1)]. During the last decade, it has become economically competitive compared to fossil fuels particularly after the recent war events in Europe[2)]. As technology has matured, the focus now is on means to improve efficiency as much as possible, which is the focus of this paper. Wind turbines are classified into two groups, horizontal axis wind turbines (HAWT)[3,4)] and the vertical axis wind turbines (VAWT).

HAWTs are well suited for large windfarms that are outside urban areas with a predominant wind direction. That is the main reason they are situated close to off/onshore or close to mountain ranges. They are more suitable for locations with high wind speed. As they are large, acoustically polluting and aesthetically unpleasant they are not suited for urban environments. On the other hand, VAWTs are well-suited for low wind speeds as they have lower startup torque requirements because of lower inertia, have a lower noise signature, and do not require large masts and landscape. The main advantage of VAWTs is their ability to operate regardless of the wind direction, making them extremely suitable to urban environments and easy to integrate in community projects[5)]. One major disadvantage of VAWT is the interaction of the rotating blades with the wakes from an upstream rotor. This interaction can lead to loss of power, increased vibration, fatigue loading, and added noise. Accounting for such effects is not possible with blade element momentum models and must be addressed with more complex CFD techniques.

VAWTs can be divided into lift-type, such as the Darrieus, and drag-type, such as the Savonius as shown in Fig. 1 [6)]. H-Darrieus straight blades are more economical and easier to manufacture than Savonius blades. VAWTs have room for improvement in self-starting, efficiency, and power consumption (active blade pitching) [7)]. Earlier research has proven that using a blade profile with a small

camber, such as the Ls0421 airfoil with a 2.4% camber ratio, can improve VAWT performance compared to a symmetrical blade profile. However, there is a lack of knowledge on the effect of blade camber alone on straight-bladed Darrieus turbines.

The aim of this study is to conduct a thorough investigation of the impact of cambered airfoils with 20% positive and negative camber, as well as a symmetric airfoil with the same thickness ratio, on the performance of straight-bladed Darrieus turbines. Using advanced numerical simulations, this research aims to supply a comprehensive understanding of the effects of different airfoil shapes on turbine efficiency, and to find the best airfoil design for increasing the performance of Darrieus turbines.

2. Brief review of VAWT development

VAWTs are suitable for limited space and urban environments since their footprint and needed spaces (both cross and downwind) between units is minimal compared to HAWT. VAWT farms can be built with very narrow spacing and that would allegedly increase the farm efficiency to have a high-power density[8]. It is also suitable for urban areas because it has high-power efficiency, and it is not sensitive to fluctuating wind direction [9].

An early attempt to improve VAWT efficiency through CFD was performed by Vassberg et al.[10] through simulation of the dynamic motion of a spinning turbine blade about a vertical axis and subjected to a uniform free-stream velocity flow field. Ferreira et al.[11] presented a systematic CFD analysis of a 2D straight-bladed rotor configuration. The influence of dynamic stall in a 2D single-bladed VAWT was examined reporting turbulence model role on the simulation accuracy.

Kumar et al.[12] developed a low Reynolds number design method for VAWT besides an optimization process using CFD to improve blade element momentum (BEM) models. Raciti Castelli et al.[13] performed a CFD study for a micro Darrieus VAWT validated with wind tunnel experimental data. It is proved the possibility of deciding the best first grid element height through statistical analysis of the Y+ parameter, to obtain maximum accuracy of the numerical prediction of rotor performance whilst keeping a sensible computational effort.

Castelli et al.[14] introduced a novel way for CFD modeling the straight-bladed VAWT offering a new design and optimization tool for predicting performance traits for turbines for which there is no test data available. In that work, the basic principles applied to BEM theory are translated to CFD allowing the correlation between flow geometric and dynamic quantities. Although the difference between the numerically calculated power curve for the turbine and the wind tunnel measurements was big, it successfully predicted the trend of the turbine.

Danao et al.[7] used CFD to study the effects of the combined effects of blade thickness and camber on a 2D model. The blades included in the study were NACA0022, NACA0012, NACA5522, and LS0421. The thinner and symmetric airfoil 0012 offered the best performance. He also pointed out the negative camber profiles produced power only on the upwind side. The study did not separate the effect of the thickness and camber, and turbine performance curves for non-design operating conditions were not provided.

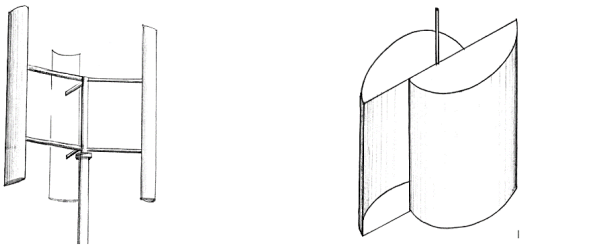

(a) Darrieus type (b) Savonius type

Fig. 1: Modern VAWT types

3. Model Description

The VAWT features three airfoils, each with a chord length of 0.246 meters and arranged 120 degrees apart from each other (shown in Fig. 2. The diameter of the rotor is set at 1.7 meters. (Diameter is radial not vertical dimension as shown in Fig. 2)

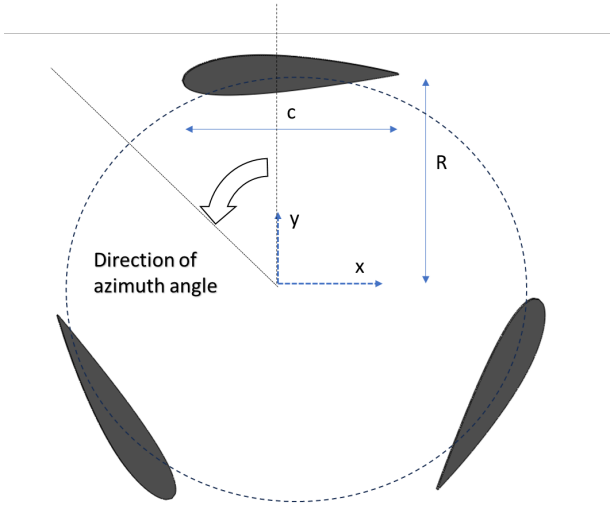

Fig. 2: A Schematic for the VAWT

In this study, the NACA 4-digit series is used to investigate the effect of camber. The profiles given by NACA 0018, NACA 2418, and negative NACA 2418 are investigated, as shown in Fig. 3.

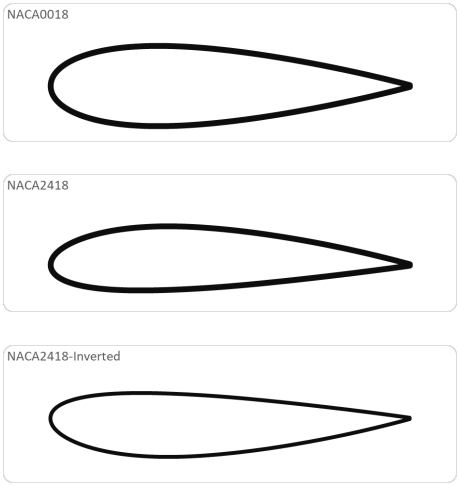

Fig. 3: Airfoil profiles comparison

4. CFD Simulation

Performing correct CFD analysis for Darrieus VAWT is challenging due to flow complexity and interaction between the up and downwind cycles of the operation[15]. 2D simulations can accurately describe the flow field and give good performance estimates when the computational domain is wide enough to simulate an open field scenario, dropping any artificial blockage effect[16].

The 2D computational domain for Darrius VAWT includes two main sub-domains, i.e., fixed, and rotating domains. Fig. 4 depicts the computational domain's main features and the imposed boundary conditions.

The fixed domain is rectangular; it stands for the physical domain extent. The inlet boundary condition is undisturbed free stream wind velocity V∞ 8 m/s. The turbulence intensity is 0.5, and the turbulence length scale is set equal to the turbine diameter. Domain outlet has atmospheric pressure. Symmetry boundary conditions are imposed on both lateral sides of the domain. A circular opening with a diameter DRR= 3.4 m equal to twice the turbine diameter is adequate for the circular rotating grid. The boundary of the circular domain is an interface condition. Domain dimensions were L1= 40D, L2 =100D, and W =60D.

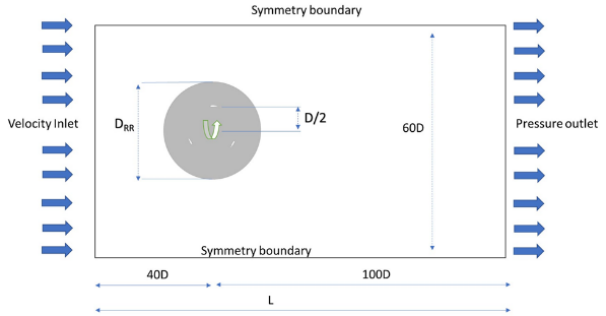

Fig. 4: An illustration of the 2D numerical domain

4.1 Validation of the numerical model

Results of the simulation study are compared to both experimental and numerical results of Balduzzi et al.[17] are shown in Fig. 5, which shows good agreement with experimental data. For λ<2, the current study results show better agreement than the reference case numerical results, which overestimated the power coefficient, Eq. 1.

$$CP = \frac{Torque(\Omega)}{0.5(\rho A U^3)} \qquad (1)$$

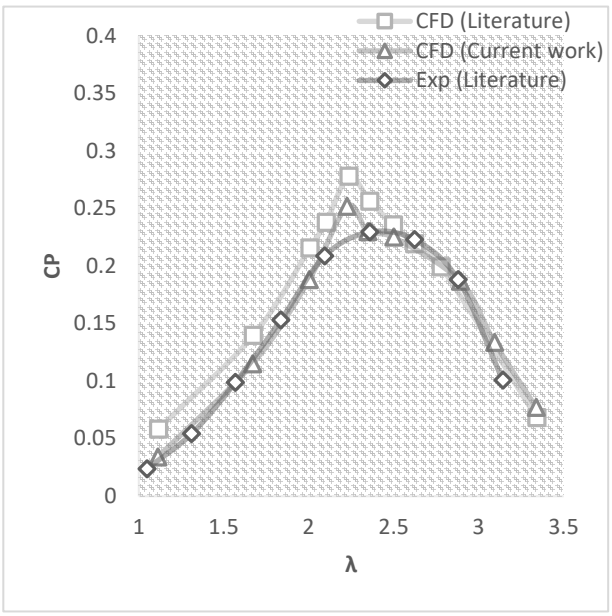

Fig. 5: Power coefficient of a VAWT calculated by CFD and wind tunnel testing by Balduzzi et al. (17)

4.2 Turbulence Modeling

There is no agreement found across the literature that suggests a specific turbulence model is best for a VAWT simulation. Special interest was put particularly on two turbulence models, namely the four-equation transition SST and the two-equations (SST) k-ω because they are popular and recommended for the problem at hand [18,19]. They are both tested to decide which is best suited for VAWT straight blade problems.

Fig.6 shows the difference between torque values from wind tunnel test conducted by Bladuzzi et. al. [17] , and CFD results. It also shows how the CFD results vary when using the four-equation transition SST and the two-equations (SST) k-ω. It is clear that SST k-ω is preferable, with a lower difference from the experiment besides being less computationally expensive. This result is consistent with results from Ref.s [17,18].

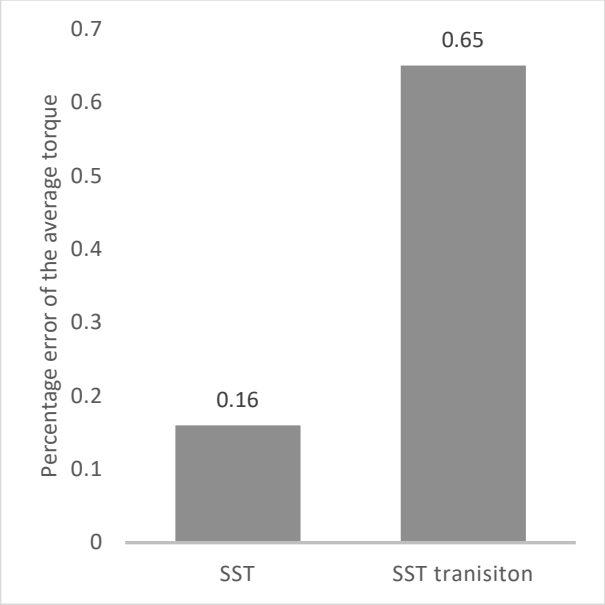

Fig. 6: Torque variation between Wind tunnel and CFD for different turbulence models when ω = 211 rpm.

4.3 Grid Sensitivity

The computational mesh is composed of two main parts: the fixed domain mesh and the rotating domain mesh, as shown in Fig. 7. Most of the mesh uses unstructured triangular elements, with an inflation layer of 50 layers surrounding the airfoils to accurately capture the boundary layer flow, resulting in a y+ value of around 1.

A close-up of the mesh structures at the leading and trailing edges is shown in Fig.9 and Fig. 10, with 604 nodes meshed on each airfoil surface. Mesh clustering was applied at the leading and trailing edges, as depicted in the figures. To control the mesh density near the blades; control circles of varying sizes were defined, as shown in Fig. 11, as suggested by Raciti et al. [13] and followed by many others such as Rossetti et al.[19], and Bianchini et al. [20]. Smooth transitions in cell sizes were implemented between the different domain meshes, with the smallest cell sizes occurring at the blade surfaces and the largest cell sizes at the domain boundaries.

A mesh sensitivity study was conducted using four mesh configurations with cell counts ranging from 130k to 460k. Fig. 12 compares the torque results for the different meshes against experimental data, the difference error range from 11.67% from the 130k grid to 0.16% from the 460k grid where it showed almost mesh-independent solution. The 460k mesh configuration was selected for its high accuracy, with a total mesh consisting of 460k elements divided into 135k cells in the fixed domain mesh and 325k cells in the rotating domain mesh.

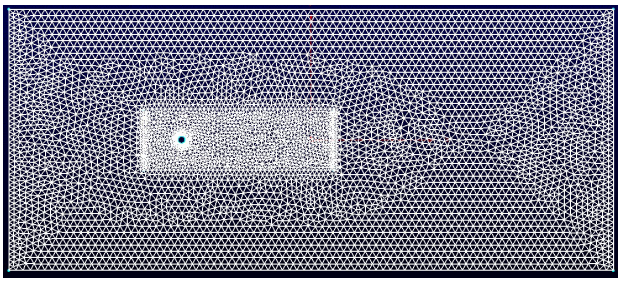

Fig. 7: Complete computational domain

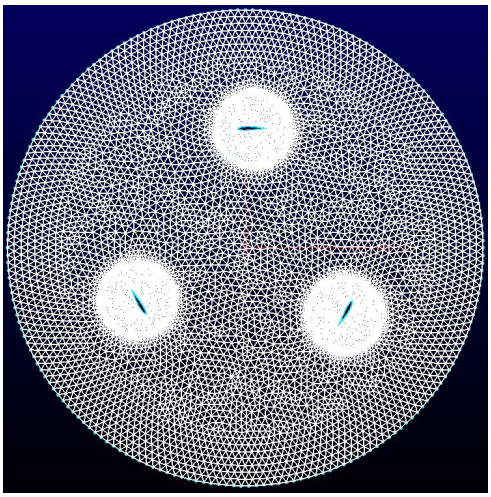

Fig. 8: Rotating domain mesh structure

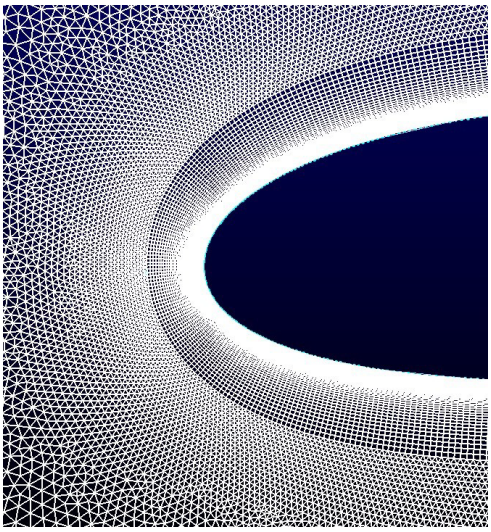

Fig. 9: Leading edge mesh structure view

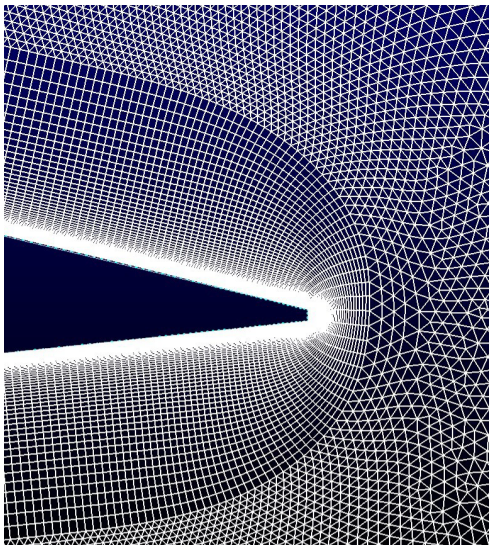

Fig. 10: Trailing edge mesh structure view

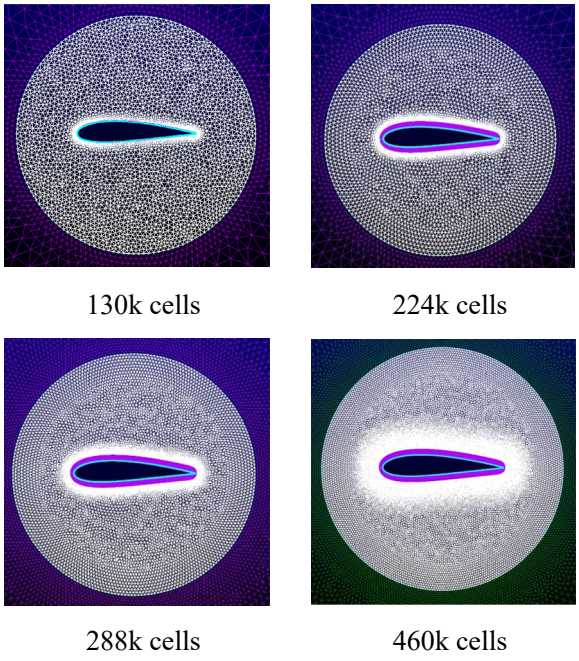

Fig. 11: Control Circle as appeared in different mesh sizes

CFD Results and Discussions

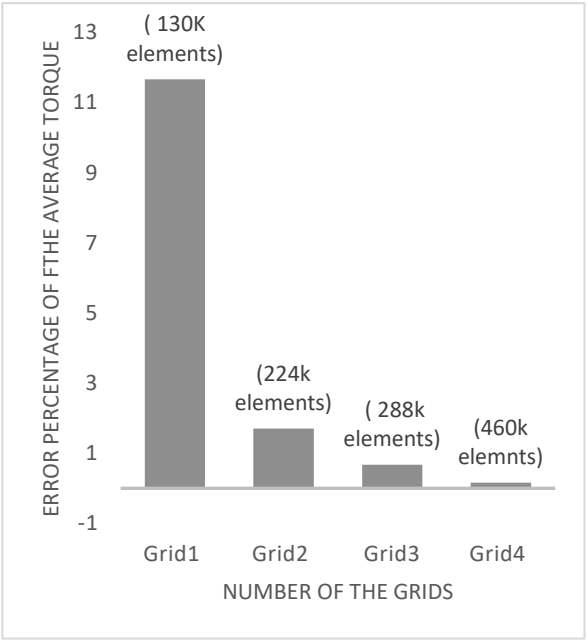

Fig. 12: Comparison between error in torque using different mesh configurations, at $\lambda = 2.3$

4.4 Solution technique (Sliding mesh vs Moving reference Frame)

There are two methods to solve fluid flow equations for vertical-axis wind turbines (VAWTs): Moving Reference Frame (MRF) and Sliding Mesh (SM). MRF models unsteady motion as steady motion using a moving frame, reducing simulation time and computational resources. SM involves moving mesh zones connected by a sliding mesh that preserves mass and momentum. Both methods were used to simulate VAWT performance, and the results showed that SM provided a better modeling of the problem, Fig. 13. However, the number of turbine revolutions needed to achieve quasi-steady configuration using SM varies from case to case. In this study, 50 revolutions at the design point were needed to achieve convergence, Fig. 14, highlighting the importance of both the sliding mesh technique and high number of revolutions to find a proper solution.

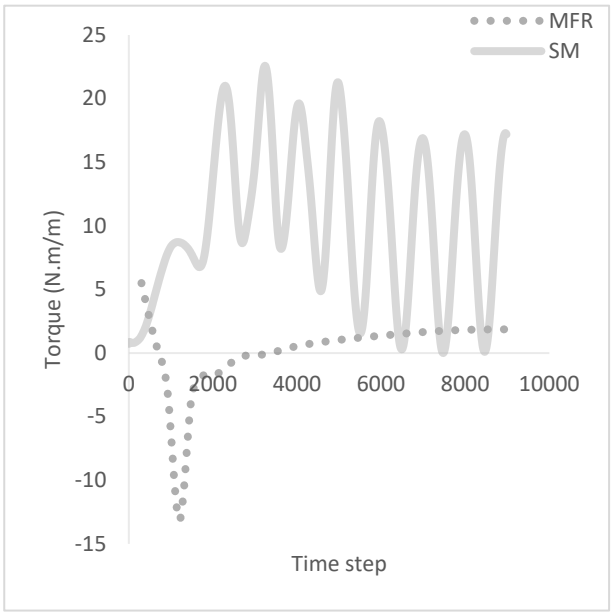

Fig. 13: Solution using Moving Reference Frame and Sliding Mesh techniques.

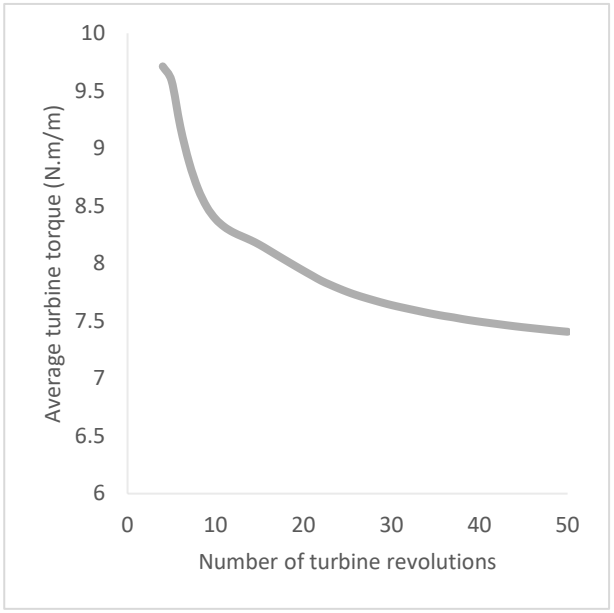

Fig. 14: Time history of turbine torque average torque from initialization till convergence

The difference in average torque between two consecutive revolutions decreases as the number of revolutions increases. It only takes 7 revolutions for the percentage difference to drop to 1%, but 50 revolutions are needed for the difference to reach 0.1%. Fig. 15 and Fig.16 show the pressure patterns behind the turbine after 7 and 50 revolutions, respectively. At 7 revolutions, the vortex shedding in the turbine's wake is still irregular and unsteady. However, after 50 revolutions, the wake flow becomes more consistent and approaches a quasi-steady state. Fig. 14 also shows that the torque difference between revolutions 7 and 50 is about 15% which justifies the excessive simulation time and resources.

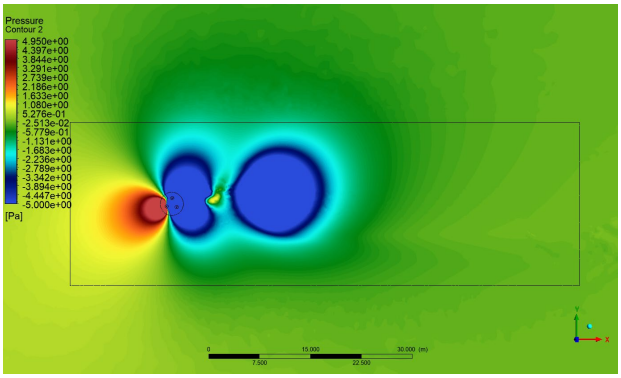

Fig. 15 : Pressure contours of the turbine's wakes after 7 revolutions

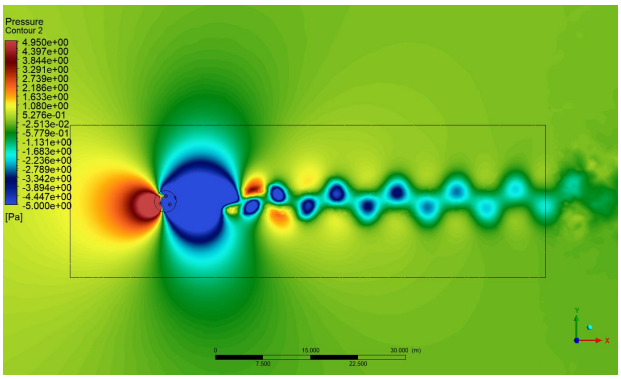

Fig. 16: Pressure contours of the turbine's wakes after 50 revolutions

4.4 Computational findings

The SST k-omega two-equation turbulence model is more correct than the SST four-equation model in predicting the performance of straight-bladed VAWT at low Reynolds numbers. This is consistent with findings from earlier studies[21]. The asymmetry of the VAWT requires a stricter convergence criterion of 0.1% to ensure accurate results, rather than the commonly used 1% as suggested by previous researchers such as C. Song et al.[22] and M. H. Mohamed et al.[23]. However, this may come at the cost of increased computational expenses.

5. Results and Discussions

5.1 Output torque and power coefficient

The performance of the VAWT when using different blade profiles is shown in Fig. 17 and Fig. 18. It is shown that the negative cambered airfoil performs worst across all tip speed ratio ranges. It also shows that in the mid-range of λ, the performance of NACA 0018 and NACA 2418 is quite similar, although the cambered 2418 has a slight advantage on both extremes of the graph. It also shows that NACA 0018 has a wider range of stable performance, but after λ exceeds 2.5 it will degrade faster than NACA 2418. The power coefficient of the rotor calculated using Eq.1 while the torque coefficient is calculated using formula in Eq. 2.

Fig. 19 shows how the output torque of a single blade changes as it rotates, using different blade shapes. The blade profiles are compared at a value of λ of 2.3. The chart shows the front half of the revolution, from 0° to 180°, and the back half, from 180° to 360°. Positive values mean the blade is generating power, while negative values mean it's losing power to the air flow. The chart shows that using a flipped NACA 2418 blade profile (compared to the standard NACA 2418 profile) results in better power generation in the range of 60° to 120°. However, the standard NACA 2418 profile loses less power in the range of 210° to 40°.

Combining the best aspect of both airfoils while rotating is feasible by using an active camber control technique such as morphing wings [24–27]. In morphing wings, the camber of the airfoil can be actively adjusted using actuators, sensors, and other smart materials. A VAWT (vertical axis wind turbine) that incorporates a morphing technique will adjust the curve of its blades at different azimuth angles to optimize torque. So a more negative camber could be used in the positive θ portion (60° to 120°) to enhance lift and reduce drag, while a less negative or even positive camber could be used in the negative θ portion (210° to 40°) to minimize power loss. It is estimated that this approach will boost the turbine's output power by 14.6%. The authors will be dedicating future work to investigating this part in detail.

$$CT = \frac{Torque}{0.5(\rho A U^2)} \qquad (2)$$

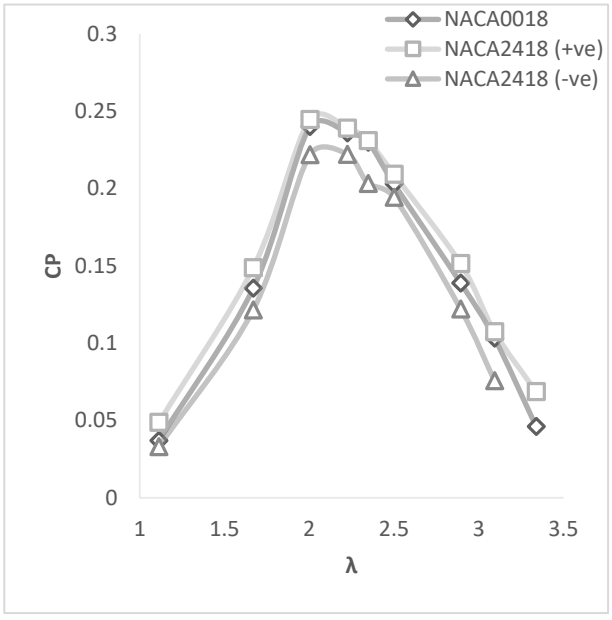

Fig. 17: Power coefficient as a function of tip speed ratio for the 3 considered blade sections.

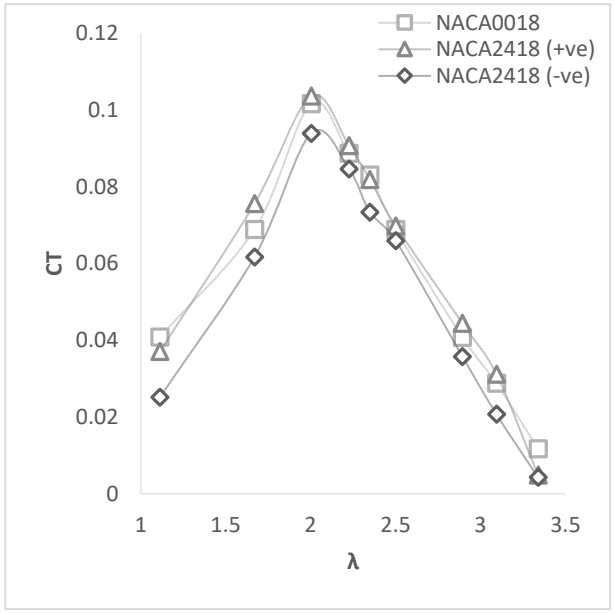

Fig. 18: Torque coefficient as a function of tip speed ratio for the 3 considered blade sections.

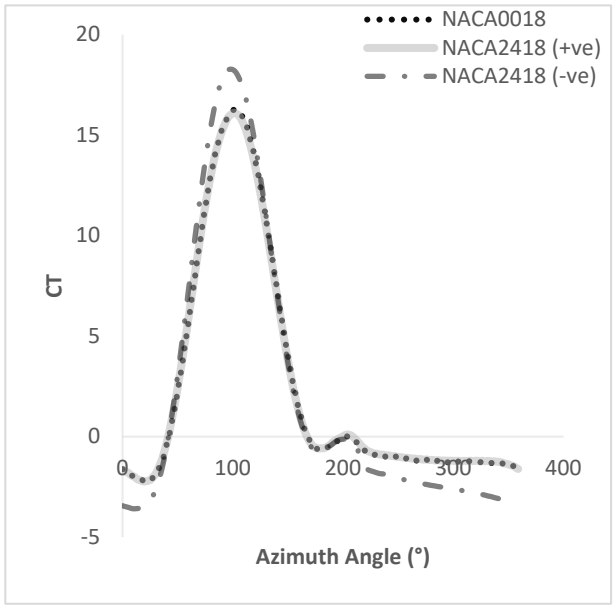

Fig. 19: Single blade torque coefficient Vs. azimuthal angle for the studied blades at λ 2.3.

6. Conclusion

Our research has revealed that negatively cambered airfoils might not be the most suitable option for practical vertical-axis wind turbines (VAWTs). The findings suggest that negatively cambered airfoils may struggle to deliver the desired output torque and efficiency levels for VAWT applications.

While negatively cambered airfoils can generate increased torque at specific azimuth angles, their overall output torque and efficiency are generally lower compared to positively cambered airfoils. This implies that, although they may excel in certain conditions, they may not be the

optimal choice for maximizing VAWT performance.

However, the implementation of a controller, such as a morphing wing technique, which enables the adjustment of the camber direction of a VAWT's blades, can significantly enhance its performance. Our research has shown that this adaptive approach can result in an improvement of up to 14.6% in overall output torque and efficiency.

Our study also highlights the importance of using a stricter convergence criterion of 0.1% to ensure accurate results in the analysis of VAWT performance. Overall, our research contributes to the understanding of the impact of airfoil shape on VAWT performance and provides insights for the development of more efficient and effective VAWT designs.

Acknowledgements

The authors are grateful to the Aeronautical Department of Cairo University for supplying valuable technical support to conduct this research project.

Nomenclature

CP	Power Coefficient
CT	Torque Coefficient
A	Frontal Area of the turbine
U	Upstream velocity
R	Radius of the turbine
c	Chord of the blade profile

Greek symbols

λ	Tip speed ratio
ρ	Air density
Ω	Rotational speed of the turbine (rad/s)

References

1) REN21, "Renewables 2021 Global Status Report," Paris: REN21 Secretariat, 2021.
2) R. Baranowski, "Wind energy benefits (fact sheet), windexchange, u.s. department of energy (doe), energy efficiency & renewable energy (eere)," 2 (2015).
3) M.M. Takeyeldein, T.M. Lazim, N.A.R.N. Mohd, I.S. Ishak, and E.A. Efkirn, "Wind turbine design using thin airfoil sd2030," *Evergreen*, **6** (*2*) 114–123 (2019). doi:10.5109/2321003.
4) M. M. Takeyeldein, Tholudin Mat Lazim, Iskandar Shah Ishak, N.A.R. Nik Mohd, and Essam Abubakr Ali, "Wind lens performance investigation at low wind speed," *Evergreen*, **7** (*4*) 481–488 (2020). doi:10.5109/4150467.
5) D. Micallef, and G. Van Bussel, "A review of urban wind energy research: aerodynamics and other challenges," *Energies*, **11** (*9*) 2204 (2018).
6) P.K. GHOGARE, "VERTICAL axis wind turbine analysis and simulation," (*August*) (2016).
7) L.A. Danao, N. Qin, and R. Howell, "A numerical study of blade thickness and camber effects on vertical axis wind turbines," *Proceedings of the Institution of Mechanical Engineers, Part A: Journal of Power and Energy*, **226** (*7*) 867–881 (2012).
8) M. Benedict, V. Lakshminarayan, J. Pino, and I. Chopra, "Fundamental understanding of the physics of a small-scale vertical axis wind turbine with dynamic blade pitching: an experimental and computational approach," *54th AIAA/ASME/ASCE/AHS/ASC Structures, Structural Dynamics, and Materials Conference*, 1–21 (2013).
9) Y. Chen, "Numerical simulation of the aerodynamic performance of an h-rotor," (*August*) 237 (2009).
10) J. Vassberg, A. Gopinath, and A. Jameson, "Revisiting the vertical-axis wind-turbine design using advanced computational fluid dynamics," *43rd AIAA Aerospace Sciences Meeting and Exhibit*, (n.d.).
11) C.J. Simao Ferreira, H. Bijl, G. Van Bussel, and G. Van Kuik, "Simulating dynamic stall in a 2d vawt: modeling strategy, verification and validation with particle image velocimetry data," *Journal of Physics: Conference Series*, **75** (*1*) (2007).
12) R. Kumar, K. Raahemifar, and A.S. Fung, "A critical review of vertical axis wind turbines for urban applications," *Renewable and Sustainable Energy Reviews*, **89** (*March*) 281–291 (2018).
13) M. Raciti Castelli, A. Englaro, and E. Benini, "The darrieus wind turbine: proposal for a new performance prediction model based on cfd," *Energy*, **36** (*8*) 4919–4934 (2011).
14) M.R. Castelli, G. Ardizzon, L. Battisti, E. Benini, and G. Pavesi, "Modeling strategy and numerical validation for a darrieus vertical axis micro-wind turbine," *ASME International Mechanical Engineering Congress and Exposition, Proceedings (IMECE)*, **7** (*PARTS A AND B*) 409–418 (2010).
15) A. Bianchini, F. Balduzzi, P. Bachant, G. Ferrara, and L. Ferrari, "Effectiveness of two-dimensional cfd simulations for darrieus vawts: a combined numerical and experimental assessment," *Energy Conversion and Management*, **136** 318–328 (2017).
16) F. Balduzzi, A. Bianchini, G. Ferrara, and L. Ferrari, "Dimensionless numbers for the assessment of mesh and timestep requirements in cfd simulations of darrieus wind turbines," *Energy*, **97** 246–261 (2016).
17) F. Balduzzi, A. Bianchini, R. Maleci, G. Ferrara, and L. Ferrari, "Critical issues in the cfd simulation of darrieus wind turbines," *Renewable Energy*, **85** 419–435 (2016).
18) F. Balduzzi, A. Bianchini, R. Maleci, G. Ferrara, and L. Ferrari, "Blade design criteria to compensate the flow curvature effects in h-darrieus wind turbines,"

Journal of Turbomachinery, **137** (*1*) 011006 (2014).
19) A. Rossetti, and G. Pavesi, "Comparison of different numerical approaches to the study of the h-darrieus turbines start-up," *Renewable Energy*, **50** 7–19 (2013).
20) A. Bianchini, F. Balduzzi, J.M. Rainbird, J. Peiro, J.M.R. Graham, G. Ferrara, and L. Ferrari, "An experimental and numerical assessment of airfoil polars for use in darrieus wind turbines—part ii: post-stall data extrapolation methods," *Journal of Engineering for Gas Turbines and Power*, **138** (*3*) 032603 (2015).
21) K. Almohammadi, D. Ingham, L. Ma, and M. Pourkashanian, "CFD sensitivity analysis of a straight-blade vertical axis wind turbine," *Wind Engineering*, **36** (*5*) 571–588 (2012).
22) C. Song, Y. Zheng, Z. Zhao, Y. Zhang, C. Li, and H. Jiang, "Investigation of meshing strategies and turbulence models of computational fluid dynamics simulations of vertical axis wind turbines," *Journal of Renewable and Sustainable Energy*, **7** (*3*) (2015).
23) M.H. Mohamed, A.M. Ali, and A.A. Hafiz, "CFD analysis for h-rotor darrieus turbine as a low speed wind energy converter," *Engineering Science and Technology, an International Journal*, **18** (*1*) 1–13 (2015).
24) H. Li, and H. Ang, "Preliminary airfoil design of an innovative adaptive variable camber compliant wing," *J. Vibroeng.*, **18** (*3*) 1861–1873 (2016). doi:10.21595/jve.2016.16705.
25) J. Sodja, M.J. Martinez, J.C. Simpson, and R. De Breuker, "Experimental evaluation of a morphing leading edge concept," *Journal of Intelligent Material Systems and Structures*, **30** (*18–19*) 2953–2969 (2019). doi:10.1177/1045389X19862369.
26) M. Baghdadi, S. Elkoush, B. Akle, and M. Elkhoury, "Dynamic shape optimization of a vertical-axis wind turbine via blade morphing technique," *Renewable Energy*, **154** 239–251 (2020). doi:10.1016/j.renene.2020.03.015.
27) Y. Zhang, W. Ge, Z. Zhang, X. Mo, and Y. Zhang, "Design of compliant mechanism-based variable camber morphing wing with nonlinear large deformation," *International Journal of Advanced Robotic Systems*, **16** (*6*) 172988141988674 (2019). doi:10.1177/1729881419886740.